May 2018

Physical and Social Systems Resilience Assessment and Optimization

Daniel Romero Rodriguez
University of South Florida, danielromero@mail.usf.edu

Physical and Social Systems Resilience Assessment and Optimization

by

Daniel Romero Rodriguez

A dissertation submitted in partial fulfillment
of the requirements for the degree of
Doctor of Philosophy
Department of Industrial and Management Systems Engineering
College of Engineering
University of South Florida

Major Professor: Alex Savachkin, Ph.D.
Mingyang Li, Ph.D.
Kingsley Reeves, Ph.D.
Kiki Caruson, Ph.D.
Alex Volinsky, Ph.D.

Date of Approval:
April 30, 2018

Keywords: Resilience Metric, Intensity Based Resilience, Social Resilience, Supply Chain Resilience, Resilience Optimization

DEDICATION

This dissertation is dedicated to my wife, parents, family, friends and professors for their support and guidance throughout these years. Their patience and constant encouragement have increased my resiliency levels.

ACKNOWLEDGMENTS

To my advisor Dr. Alex Savachkin for his patience and guidance from the selection of the research topic to the development of our research objectives. To all faculty members and staff at IMSE USF for their example of professionalism and passion.

TABLE OF CONTENTS

LIST OF TABLES

LIST OF FIGURES

ABSTRACT

Resilience has been measured using qualitative and quantitative metrics in engineering, economics, psychology, business, ecology, among others. This dissertation proposes a resilience metric that explicitly incorporates the intensity of the disruptive event to provide a more accurate estimation of system resilience. A comparative analysis between the proposed metric and average performance resilience metrics for linear and nonlinear loss and recovery functions suggests that the new metric enables a more objective assessment of resilience for disruptions with different intensities. Moreover, the proposed metric is independent of a control time parameter (usually denoted as T^* or T_{LC} in the average performance metrics). This provides a more consistent resilience estimation for a given system and when comparing different systems.

The metric is evaluated in the study of community resilience during a pandemic influenza outbreak and the analysis of supply chain resilience. As a result, the model quantifies constant, increasing and decreasing resilience, enables a better understanding of system response capabilities in contrast with traditional average performance resilience metrics that always capture decreasing resilience levels when the disruptive events magnitude increases. In addition, resilience drivers are identified to enhance resilience against disruptive events.

Once resilience drivers have been found, then a multi-objective resource allocation model is proposed to improve resilience levels. Previous resilience optimization models have been developed mainly based on a single resilience metric. The existing bi-objective models typically maximize resilience while the recovery cost is minimized. Although the single metric approach improves system resilience some of their limitations are that

the solution is highly dependent on the selected resilience index and generally few optimal points are found. To overcome the rigidity of a unique metric a bi-objective model is proposed to maximize two key resilience dimensions, the absorptive and restorative capacities. This approach has the potential to offer multiple non-dominated solutions increasing decision makers alternatives where the single metric solutions are included.

1 INTRODUCTION

Events such as natural disasters, deliberate attacks, or random failures may interrupt a system's operations causing costly, long lasting consequences thus highlighting the need for resilient systems [1, 2]. Systems' ability to withstand and recover from disruptive events while delivering a desired outcome is a widely accepted general definition of system resilience [3, 4, 5]. The concept of resilience has been studied on social [6, 7], physical [4, 8], cyber [9] and interdependent systems [10, 11].

To understand and improve this important property, decision makers need an accurate measurement of resilience, which has proven to be a challenging task given the broad variety and complexity of systems and disruptive events. Several fields of science have proposed resilience estimators without a general agreement for a unified metric or a consistent approach [5]. Among the proposed quantitative resilience metrics in social and physical systems, this property has been quantified as a composite index based on multiple social indicators [1] , the average performance [12], probability to absorb and recover from a seismic event [13], time dependent recovery rate [14], and system response capabilities product [15]. While these models contribute to the understanding of system resilience, there is not a clear connection of the resilience capability with the disruptive event magnitude.

Most resilience metrics found in the literature incorporate two main system's abilities: to absorb the shock from a disruptive event and to recover from it [3, 4]. However, these abilities have not explicitly been related to the disruption intensity (or magnitude). This can lead to an underestimation of resilience for disruptions with higher intensities. Aver-

age performance or resilience triangle metrics [12, 8, 16] are prone to this effect, where as the disruption magnitude increases, the resilience invariably decreases.

In the social science context the vast majority of studies develop qualitative tools to explore individual or community resilience. For instance, in psychology [17] and ecology [18] surveys are collected to assess resilience levels. There is a lack of agreement on how to assess social resilience, the challenge remains to develop quantitative metrics that can be implemented across systems and research areas.

Resiliency has been considered a key property in public health to enhance community response while facing natural disasters and pandemic outbreaks [19]. Even though this term has been discussed in public health, an operational resilience metric based on community response variables and disruption intensity has not been proposed or implemented. Thus, the goal is to develop and implement an operational metric to assess and improve social systems resilience.

Resilience improvement tools, such as resource allocation models, guide decision makers towards the resilience dimension where investment is required to boost performance and minimize disruptive events consequences [20]. These strategic models enable investment prioritization when multiple hardening and recovery actions are available. For instance, in the disaster management field there has been developed a significant number of resource allocation models to harden [21, 22] and restore [23, 24, 25] a system while facing natural disasters or man-made attacks. Therefore, the existence of strategic resource allocation to increase resilience levels is critical to assist decision makers in the strategies selection that will maximize resilience capabilities.

The main contributions in this research are a new intensity based resilience metric, the application of this metric in physical and social systems, the identification of resilience drivers, and the development of static budget allocation models to minimize the absorptive and restorative capacities.

This dissertation is organized as follows: Chapter 2 presents the literature review section that analyzes common resilience metrics found in engineering and social sciences disciplines, resilience drivers identification, and optimization models to boost resilience. Chapter 3 describes the overall and specific research objectives. Chapter 4 presents an intensity based resilience metric. The metric is analyzed for several classes of linear and nonlinear loss and recovery functions and the resulting resilience is compared to that of common average performance metrics. the metric is tested on social and physical systems. Chapter 5 explores the identification of resilience drivers in social systems. Then, Chapter 6 proposes static multi-objective optimization models to improve resilience levels Finally, Chapter 7 discusses the key findings and future research.

2 LITERATURE REVIEW

The literature review chapter analyzes existing quantitative resilience approaches that have been used in engineering and social sciences disciplines. Then, a discussion is conducted about the models in social and physical systems to identify resilience drivers. The next section, explores static optimization models that have been implemented to improve resilience.

2.1 Resilience Metrics

The first resilience metric can be traced back to 1845, used in mechanical engineering, to test a material's capacity to absorb energy during compression and elongation tests [26]. Since then, resilience of a material has been measured as a function of the deformation ϵ and the maximum strength σ before the material permanently deforms (see Eq. 2.1).

$$R = \frac{\sigma\epsilon}{2} \tag{2.1}$$

In the 70's, the term *resilience* was revisited in ecology and defined as "the measure of the persistence of systems and of their ability to absorb change and disturbance and still maintain the same relationships between populations or state variables " [27]. Two noteworthy metrics were proposed in this study. The first metric is the probability that a system will leave a set of states where it delivers expected outcomes. The second metric is the force required to make a system leave an equilibrium state.

The event magnitude or intensity has since been recognized as an important factor that should be considered in any resilience study [28]. This factor is usually referred to as the external disturbance and it is a recurrent consideration in environmental sciences.

Most recent approaches have included multiple dimensions or system capabilities to measure resilience. In civil engineering, Bruneau et al. [12] proposed four dimensions for physical and social systems: robustness, redundancy, resourcefulness, and rapidity. In the economics science, Rose [29] defines static and dynamic resilience. In systems engineering, Francis and Royce [15] define three resilience capacities: absorptive, adaptive, and recovery/restorative. In evaluating the dimensions (capacities) listed above, it is possible to group most of them in two sets. The first set includes the capacities that contribute to the initial loss of performance, such as robustness, static resilience, or absorptive capacity. The second set refers to the recovery dimension, which includes the rapidity, dynamic resilience, or restorative capacity.

Although the resilience metrics have been developed using similar dimensions or capacities, their interpretation and decision support applicability differ. In what follows, we review four broad classes of metrics: i) average performance metrics, ii) multi-dimensional metrics, iii) time-dependent metrics, and iv) probability based metrics.

In the first group, known as *average performance* or *resilience triangle metrics*, a system's resilience is measured as the average performance between the time a disruption occurs until the moment of system's recovery. The main idea was introduced by Bruneau et al. [12] to measure infrastructure resilience under seismic events. An extended version of this formulation is shown in Eq. 2.2, where $Q(t)$ is the performance function at time t, T_{OE} is the time of the event occurrence, and T_{LC} is the control time [8].

$$R = \int_{T_{OE}}^{T_{OE}+T_{LC}} \frac{Q(t)}{T_{LC}}\, dt \tag{2.2}$$

Using an equivalent notion, Zobel [16] developed a model to estimate resilience assuming a linear recovery. In this metric (Eq. 2.3), X is the initial performance loss, T is the recovery time, and T^* is the study period or control time.

$$R = 1 - \frac{XT}{2T^*} \tag{2.3}$$

Among average performance metrics, the model proposed by Ayuub [30] accounts for the preparation and recovery stages in a probabilistic context, which allows a flexible and accurate modeling of complex scenarios [4]. In this formulation (Eq. 2.4), T_i is the time of the failure occurrence, ΔT_f is the disruptive event duration, ΔT_r is the recovery time, F is the failure profile, and R is the recovery profile.

$$Resilience(R_e) = \frac{T_i + F\Delta T_f + R\Delta T_r}{T_i + \Delta T_f + \Delta T_r} \tag{2.4}$$

The resilience triangle approach has been extended to include multiple disruptive events [31, 32], stochastic behaviors [30], system interdependence [33], and nonlinear recoveries [8]. These extensions provide higher flexibility when fitting performance functions.

A resilience triangle metric has been implemented as an objective function in an optimization model for resource allocation to maximize resilience levels [34]. A similar approach was developed by Miller-Hooks et al. [35], where a two-phase optimization model maximized the average performance resilience from Eq. 2.5, based on the satisfied demand before (D_i) and after (d_i) a disruptive event. Resilience based budget allocation in preparedness and recovery stages for disrupted air transportation networks was considered by Janic [36].

$$R = \frac{E(\sum d_i)}{\sum(D_i)} \tag{2.5}$$

Average performance resilience metrics have been widely accepted due to the ease of their interpretation. A common limitation in equations (2.2) and (2.3) is the use of subjective, expert based parameters, such as the time of analysis or control time. Such subjectivity affects the accuracy of resilience measurement for a single system and comparisons between two or more systems.

In the *multi-dimensional class of metrics*, two or more resilience dimensions are combined by a linear combination or multiplication. The former case has been commonly used in community disaster management [37, 38], where principal component analysis is performed on a set of metrics to detect correlations. The principle metrics are then transformed to an equivalent scale whereby their aggregation using a linear combination becomes possible. An integration of metrics using a multiplication occurs when two or more dimensions are multiplied to obtain a single index (e.g., [15], see Eq. 2.6). In this case, resilience is the product of three resilience dimensions, where S_p is the speed recovery factor, F_r is the performance at a stable recovered state, F_d is the performance at a disrupted state, and F_0 is the initial system performance.

$$R(S_p, F_r, F_d, F_0) = S_p \frac{F_r}{F_0} \frac{F_d}{F_0} \tag{2.6}$$

The main advantage of this class of metrics is that the resilience concept has a multi-dimensional nature brought by dimensions of similar kind. This structure enables the model to integrate more resilience dimensions as needed by decision makers. However, aggregation of variables oftentimes presents challenges in the outcome interpretability due to the resulting metric units and possible lack of physical meaning.

Time dependent metrics view system resilience as a function of time [14] (see Eq. 2.7). In this formulation, the performance function is measured at different times to estimate the level of improvement up to time t. The model parameters for a disruptive event e_j are the initial state performance $F(t_0)$, the performance level at the disrupted state $F(t_d|e_j)$, the

performance at the recovered state $F(t_r|e_j)$, and the performance level at time t_r , where $t_r \in (t_d, t_f)$.

$$R(t_r|e_j) = \frac{F(t_r|e_j) - F(t_d|e_j)}{F(t_0) - F(t_d|e_j)} \tag{2.7}$$

The above model has been extended and implemented to waterway networks [39] and container terminals [5].

The class of time dependent metrics also includes variations of resilience triangle formulations, such as [11]. In this model (see Eq. 2.8), P_T is the targeted performance curve and P_R is the real performance curve.

$$R(T) = \frac{\int_0^T P_R(t)dt}{\int_0^T P_T(t)dt} \tag{2.8}$$

Probability based metrics quantify system resilience as a probability. The first such metric was defined as the odds that a system will remain in an equilibrium state or basin after a disturbance [27]. The original formulation did not include the restorative capacity; it was added later when an equivalent metric was defined as the probability that the system's loss will be less than the maximum loss (X^*) and the system will recover faster than the maximum time to recover (T^*) for a given earthquake [13]. A similar model was defined as the probability that a system will reach a set of viable states before a pre-specified time [40].

$$P(A|I) = P(X_0 < X^*, T_1 < T^*) \tag{2.9}$$

Equation (2.9) measures resilience for a given single scenario; it has been extended to include probabilities of different disruptive events, see Eq. 2.10, to calculate the total probability (i.e., resilience).

$$R = \sum P(A|I) * P(I) \tag{2.10}$$

The above formulation suggests to simulate disruptive scenarios with multiple replications in order to measure if the system satisfies the resilience conditions for X and T.

In the design of engineered systems, Youn et al.[41] used a probability based resilience as a function of a system's reliability and restoration capabilities, see Eq. 2.11 (symbol Ψ was used to denote resilience since symbol R was reserved for reliability). In this formulation, P_{Diag}, P_{Prog}, P_{Corr} are the diagnosis, prognosis, and correction probabilities, respectively. This idea has been extended to measure resilience as a time dependent probability [42].

$$\Psi = R + (1 - R)P_{Diag}P_{Prog}P_{Corr} \tag{2.11}$$

The probability based resilience metrics have been extended to use bayesian networks to capture contributions of individual system components and variables to the overall resilience [43, 44].

Probability metrics have been widely used in the design and analysis of physical systems. The main benefit of these models is a relative ease of interpretation.

The review of the existing system resilience metrics has shown that most of the models include common dimensions of absorptive and restorative capacities or their equivalents. The magnitude or intensity of a disruptive event has been identified as a relevant factor [8] but it has not been explicitly incorporated in a resilience metric.

2.1.1 Social Systems Resilience Metrics

Resiliency in social systems has been measured trough multiple indexes or composite metrics. Cutter [38] combines economic, social, institutional, infrastructure and community capital factors into a single resilience metric to assess system ability to cope with disasters. A similar approach is developed by Asadzadeh et al. [37], where 36 indicators are evaluated and aggregated in a disaster resilience index. Magis (2010) [45] defines community resilience by eight dimensions that include community resources and strategic action, where each dimension is defined by multiple metrics. Equivalent methodologies are

developed [46] and implemented to assess multiple indexes and select the most important from the resilience perspective [47]. Even though these approaches capture multiple resilience capabilities, system response variables when a disruptive event strikes are not included in the analysis.

Resilience in public health during a pandemic outbreak has been explored mainly by using qualitative tools. These studies include the analysis of health education training [48] and authorities communication with the community to increase resilience [49]. There is an indirect study of the productivity loss in different industries after a pandemic outbreak [50] where resilience is captured using an index developed to measure the interdependency recovery rate for multiple industries when a disruptive event strikes [51]. In the review of quantitative metric in public health, no implementations of resilience metrics were found besides the analysis based on the infection attack rate (IAR).

2.1.2 Supply Chain Resilience Metrics

The metrics to assess resilience in a supply chain are divided in qualitative and quantitative. In the first group surveys and experts' opinions are captured to assess system resilience level. For instance, a deterministic supply chain resilience index (SCRI) is proposed based on nine resilience enablers, such as agility, collaboration, visibility, among others [52]. Similarly, the supply chain resilience assessment and management (SCRAM) [53] is suggested to measure system resilience by measuring twelve capabilities [54]. The importance of these qualitative tools is their ability to establish how significant are strategic drivers or enablers in the overall system resilience performance.

In the second group, the quantitative metrics are divided in two categories: i. average performance and ii. multiple dimensions .

The average performance metrics measure system performance over a pre-fixed time after a disruption has affected the system [12]. A linear approximation [16] is adapted and

implemented in the design of a global supply chain affected by suppliers disruptions [55]. This approach has been widely extended [30, 56] and implemented in diverse contexts [4].

An equivalent metric based on system expected performance after a disruptive event has been proposed on transportation networks analysis [35] and implemented to measure supply chain resilience [57].

The multiple dimensions category includes metrics that are either a combination of factors into a single value or a set of multiple indexes. In the former case, an initial model of node resilience in logistic networks is estimated as a function of supply reliability, resources availability, and reachable deliveries [58]. A second model, includes five dimensions from a system disruption profile and unifies these response variables based on their weights and echelon position [59]. A third general metric integrates system restorative, absorptive and adaptive capacities to quantify resilience levels [15].

In the multiple metrics case, a three metrics framework is proposed to diagnose network resilience based on the largest connected component size, average and maximum path length [60]. Alternatively, in supply chain design eleven indicators are measured to evaluate system resilience and overall performance [61].

2.2 Resilience Drivers

The importance of the identification of system resilience drivers is that enables the improvement of the resilience levels. In this subsection, the review is focused on how these drivers have been estimated in public health and supply chain analysis.

2.2.1 Community Resilience Drivers in Public Health

In public health, high resilience levels to pandemic outbreaks are connected to communication, trust, willingness to take responsibility and commitment to prepare [49, 62]. Other studies analyze system capabilities that are part of community resilience, for instance an ANOVA design is evaluated in a simulation model to estimate the impact of

non pharmaceutical interventions in the IAR [63]. Similar analysis have been performed to estimate the impact of pharmaceutical interventions [64, 65].

Resilience drivers in social systems are estimated using different statistical tools. Cutter et al. (2010) [38] normalize multiple indicators by using min-max rescaling and assign equal weights when aggregating the indexes. A case study in Theran implements a composite resilience metric based on hybrid factor analysis and analytic network process [37]. These studies do not focus on the absorptive and restorative capacities.

The studies of resilience drivers identification in social systems do not include response variables or are focused on a single resilience capacity. There is a need to estimate resilience drivers that involve at least two factors: the absorptive and restorative capacities.

2.2.2 Supply Chain Resilience Drivers

The review of supply chain resilience drivers divides the analysis on strategic drivers based on qualitative studies and operational drivers based on system tactical and operational policies.

A summarized list of the strategic factors that build supply chain resilience include the following drivers: Agility, flexibility, collaboration, redundancy, visibility, integration, information sharing, network topology, and risk management [66, 67, 68]. Even though these drivers provide a general guideline to improve system resilience, due to their strategic nature they are not easily connected with operational variables that may impact system resilience.

On the contrary, the relationship between resilience and operational variables have been less explored. Inventory levels benefit system performance upon demand uncertainty [69].

2.3 Resilience Optimization Models

The review studies optimization models that have been implemented to maximize system resilience. The discussion includes single and multi-objective models.

In the single objective group, the implementation of the average performance or equivalent functions are common to allocate resources targeting resilience improvement. A linear approximation of the performance function was tested while evaluating multiple allocation functions and uncertainty in model parameters [34]. This model is implemented in the Katrina case study where linear, exponential, quadratic and probability based models were tested. The allocation model is extended to include dynamic resource allocation [20].

An equivalent resilience metric to the average performance measures the ratio of network performance before and after a disruption [35]. A representative showcase of optimization models using this metric includes the study of trans-oceanic communication cable [70], transportation networks [71, 35] and network topology analysis [72]. This metric has been applied widely in network resilience analysis.

Other single objective studies include a cost function in supply chain management, where resilience indicators related to network design are suggested to be included as part of the objective function or model constraints [61]. Logistic network resilience is measured and improved as a function of nodes redundancy, supplier and distribution reliability [58]. A multi-level framework is developed to design complex engineered systems where resilience is placed at the top level [41].

Single objective models maximize resilience based on authors' metric paradigms or preferences, but there are no comparison among different resilience metrics to verify the dependency of the optimal solution with the variety of metrics.

The multi-objective group contains mainly bi-objective models where the objectives are resilience and cost. These models have been applied in supply networks [55, 57]

and retrofit bridge analysis [73]. This type of model was suggested as a possibility in waterway networks study to maximize resilience and minimize the recovery cost when selecting a set of restoration actions [39]. The inclusion of the cost in resiliency analysis highlights the importance of the resources spent to harden and recover the system.

Within this group others models have used more than two objectives. For instance, in the analysis of restoration strategies in interdependent infrastructure individual resilient metrics are considered for each system, this framework is implemented in power and gas networks [11]. A socioeconomic and engineering methodology is proposed to improve community seismic resilience [74]. This framework is implemented to evaluate seismic retrofit plans via an optimization model where the objective functions are economic loss, the number of morbidities, recovery time and the seismic retrofit plan cost [75].

Table 2.1 displays a comparison of the resilience optimization models based on the number of objectives, model structure, and solution procedure. It is observed that Mixed Integer Programs (MIP) were the most common models. In the case of solution procedures, genetic algorithms were extensively implemented in multi-objective problems. While there are multi-objective models that include resilience, they dedicate a single objective to resilience, making the models dependent to an specific metric. We expect to benefit from the multi-objective structure by adding as many objective functions as resilience capacities are analyzed to avoid dependence of a single metric and provide same importance to all the dimensions.

The gaps that were identified from this review can be summarized as follows: i. Models are dependant to specific resilience metrics, which can lead to bias and limit the implementation in other applications. This will be addressed by proposing models that are built based on critical resilience dimensions. ii. Disconnection between resource allocation models and overall system resilience. Few models provide a strategic standpoint to allocate resources based on overall resilience. Models should be intended to connect tactical resource allocation with system resilience. These gaps are going to be solved by

Table 2.1: Literature review resilience optimization models

Research Article	**Objectives**		**Model**	**Solution Procedure**
	Single	Multiple		
[58]	✓		Non-structured	Genetic algorithm
[70]	✓		MIP	Branch and bound
[41]	✓		MINLP	Genetic algorithm
[71]	✓		Stochastic MIP	Benders decomposition and Column generation
[73]		✓	MIP	NSGA-II
[39]	✓		Combinatorial	Heuristic
[35, 72]	✓		Stochastic NLP	L-shaped method
[61]	✓		MIP	Branch and cut
[11]		✓	Non-structured	Genetic algorithm
[76]	✓	✓	MIP	Box algorithm
[55]		✓	Two-stage stochastic	ϵ-constraint
[57]		✓	MIP	NSGAII-Co-Kriging
[20]	✓		NLP	Analytical
[22]		✓	Two-stage robust optimization	Column and constraint generation
[75]	✓		NLP	Analytical

proposing a new intensity based resilience metric, the identification of systems' resilience drivers, and multi-objective optimization model to maximize resiliency levels.

3 RESEARCH OBJECTIVES

The overall research objective is to develop new models for resilience of physical and social systems which incorporate disruption intensity, identify resilience control factors and optimize resiliency. These are the specific research objectives:

- Develop resilience assessment models that incorporate disruption intensity. The quantitative models will capture resilience relative to the disruptive event intensity, which provides a fairer comparison in contrast with the average performance metrics. These metrics are evaluated in physical and social systems.

- Identify resilience control factors. A previously validated agent based simulation model is implemented to study the community response to pandemic influenza outbreaks. The response variables time to recover and performance loss are measured for different virus strengths and non pharmaceutical interventions. Then, regression models are deployed to identify relationships among intervention policies and system resilience capabilities. An equivalent analysis is carried out in a supply chain to identify the system policies and the relationship with resilience.

- Develop multi objective optimization models for allocation of resilience resources. Static models are proposed to ensure optimal resource allocation that maximize systems resilience levels. Multiobjective LP and MIP models are compared with single objective resilience models. Then, the multiobjective models are implemented in the social system testbed to identify the best strategies to maximize resilience while balancing social impacts.

4 INTENSITY BASED RESILIENCE METRIC

When measuring a system's resilience, the system's response to a disruptive event needs be analyzed relative to the disruption intensity. A system which responds by a smaller loss of performance to a disruption with a higher intensity should be viewed as having a higher resilience. In what follows, the suggested metric includes three elements: absorptive capacity, restorative capacity, and the disruption intensity.

4.1 $R(I)$ Metric

Most of the existing metrics assume that the initial performance loss X and the recovery time T are independent [16, 30]. In this research it is assumed that the recovery time is dependent on the initial performance loss.

We first propose that the absorptive capacity R_X be measured as the disruption intensity I dissipated per unit of the performance loss X, as below:

$$R_X = \frac{I}{X} \tag{4.1}$$

Similarly, the restorative capacity R_T is measured as the disruption intensity dissipated per unit of recovery time T:

$$R_T = \frac{I}{T} \tag{4.2}$$

The system resilience is then measured as the product of the absorptive and restorative capacities from Eq. 4.1 and 4.2:

$$R = \frac{I^2}{XT} \tag{4.3}$$

The above general model in Eq. 4.3 estimates system resilience relative to the disruption intensity. This allows a comparison of the resilience of different system designs to a given disruptive event. At the same time, identification of the performance loss function $X(I)$ and the recovery function $T(X(I))$ aids decision makers in understanding of their system resilience in order to take reactive and proactive actions to improve the system response for different disruptive events.

In the following sections, we analyze the proposed metric for different forms of $X(I)$ and $T(X)$. In the case of $X(I)$, most existing models assume either an instantaneous performance loss (e.g., observed after a natural disaster [16]) or a gradual (continuous or stepwise) loss [14]. Recovery functions have attracted more attention whereby most models consider either linear [16] or nonlinear trajectories [8, 32]. We will consider both cases in our analysis of the proposed metric.

In the linear case we assume that $X(I)$ and $T(X(I))$ are linear functions so that the system response is linearly proportional to the disruption intensity (See Eq. 4.4 and 4.5). The linearity assumption can hold as an approximation in situations where the absorptive and restorative rates do not vary substantially during the analysis period. Some resilience metrics assume linearity [16] and this scenario is included as a special case of the nonlinear scenarios discussed later.

In Eq. 4.4 and Eq. 4.5 below, the parameters α and β are rates that measure a system's ability to absorb and recover from a disruptive event respectively. We assume that these parameters are constant throughout the disruption and recovery processes (time varying rates will be considered in our future work).

$$X = \alpha I \tag{4.4}$$

$$T = \beta X \tag{4.5}$$

In Eq. 4.4 and 4.5, the importance of α, the unit loss per disruption intensity, and β, the recovery rate, is that they can serve as controls or drivers of a system's resilience (see Eq. 4.6 and 4.7), whereas X and T should be viewed as response variables.

$$\alpha = \frac{X}{I} \tag{4.6}$$

$$\beta = \frac{T}{X} \tag{4.7}$$

Based on Eq. 4.4 and 4.5, the resilience metric becomes as follows:

$$R = \frac{1}{\alpha^2 \beta} \tag{4.8}$$

The above result in Eq. 4.8 suggests that when a system absorbs and recovers at the same respective rates for different disruption intensities, its resilience remains constant and independent of the actual value of I. Therefore, an increase in the performance loss does not necessarily imply a lower resilience, as for average performance metrics.

In the nonlinear case at least one of the functions $X(I)$ or $T(X)$ is nonlinear. Such cases have been widely discussed in the resilience literature where multiple recovery profiles are included [77, 78]. We assume that $I > 1$ to generalize the system behavior in the non linear scenarios. Our analysis includes the following cases: (a) general nonlinear functions with positive real exponents, and (b) logarithmic and exponential functions.

(a) General nonlinear functions

In the general nonlinear case, both $X(I)$ and $T(X)$ are nonlinear (see Eq. 4.9 and 4.10), where parameters n and m are positive real numbers:

$$X = \alpha I^n \tag{4.9}$$

$$T = \beta X^m \tag{4.10}$$

It then follows that when the two response variables are nonlinear the general resilience equation is given by the following expression:

$$R = \frac{I^{2-n(1+m)}}{\alpha^{m+1}\,\beta} \tag{4.11}$$

The above equation reduces to Eq. 4.8 when $n = 1$ and $m = 1$. Assuming a linear recovery when $m = 1$, we discuss two sub-cases that lead to different system response: $n > 1$ and $0 < n < 1$.

When $n > 1$, as I increases, the absorptive and restorative capacities decrease and so does resilience. This case is characterized by higher sensitivity of resilience to disruption intensity. Such behavior can be observed in systems that absorb shocks relatively well up to a certain level of intensity; once the level is exceeded, the system "gives in" and its resilience degrades at an increasingly increasing rate. This pattern can be observed, for instance, in networks with some nodes having high connectivity or cyclicity [79] - once such a node fails, it will cause cascading failures of its dependent subnetwork.

When $0 < n < 1$, system resilience is less sensitive to variations in I. Since resilience improves as I increases, this model can be used for systems which can adaptively sustain disruptions of higher magnitude, up to a certain level. Such dynamics can be observed in adaptive networks which learn or develop mechanisms to cope with shocks. One example is the effect of herd immunity in communities affected by pandemic outbreaks of infectious diseases.

When $0 \leq n, m < 1$, both the absorptive and restorative capacities progressively improve as I increases, which results in progressively higher resilience. On the other hand, when $n, m > 1$, the absorptive and restorative capacities get progressively worse, which makes resilience decrease. In general, for any combination of n and m, depending on the sign of the exponent $2 - n(1 + m)$, there will be three shapes of the resilience curve, as I increases: increasing (positive exponent), decreasing (negative exponent), and constant (zero exponent).

(b) Logarithmic and exponential functions

We first assume that $T(X)$ is linear with respect to X and the loss function has a nonlinear structure of the following form:

$$X = \alpha\, ln(1 + I) \tag{4.12}$$

The resilience metric for the logarithmic case based on Eq. 4.12 is given by the following equation:

$$R = \frac{I^2}{\alpha\beta\, ln(I)^2} \tag{4.13}$$

In this case (see Eq. 4.13), as I increases, resilience increases as well, which resembles the general nonlinear case for $0 < n < 1$.

When the performance loss function has an exponential form (see Eq. 4.14),

$$X = \alpha\, e^I, \tag{4.14}$$

system resilience has the following form:

$$R = \frac{I^2}{\alpha^2\beta e^{2I}} \tag{4.15}$$

This case (see Eq. 4.15) follows the same pattern as the general nonlinear case for $n > 1$: resilience decreases as I increases.

From the above cases, it can be seen that the proposed model can accommodate constant, decreasing, and increasing resilience dynamics, depending on the relationships among X, T and I. The ability to capture such interactions increases the flexibility of the metric since in the previous models X and T were assumed independent and I was not considered.

In order to compare the proposed intensity based metric R(I) with the average performance (AP) metric from Eq. 2.3, Table 4.1 was developed for the linear and nonlinear cases considered above. From the table 4.1, for each case, the resilience for the average

Table 4.1: Metrics comparison

Case	R(AP)	R(I)
Linear $X = \alpha I$ $T = \beta X$	$1 - \frac{\alpha^2 \beta I^2}{2T^*}$	$\frac{1}{\alpha^2 \beta}$
General $X = \alpha I^n$ $T = \beta X^m$	$1 - \frac{\alpha^{m+1} \beta I^{n(m+1)}}{2T^*}$	$\frac{I^{2-n(1+m)}}{\alpha^{m+1}\,\beta}$
Logarithmic $X = \alpha\, ln(1+I)$ $T = \beta X$	$1 - \frac{\alpha^2 \beta ln(1+I)}{2T^*}$	$\frac{I^2}{\alpha\beta\, ln(I)^2}$
Exponential $X = \alpha\, e^I$ $T = \beta X$	$1 - \frac{\alpha^2 \beta e^I}{2T^*}$	$\frac{I^2}{\alpha^2 \beta e^{2I}}$

performance metric is a decreasing function of I. This follows since the average performance is proportional to the performance loss, which invariably decreases as I increases, regardless whether the restorative and/or absorptive capacities remain constant or increase. This highlights the main difference between the two metrics such that the proposed model captures more complex interactions among X, T, and I.

4.2 Numerical Examples

Numerical examples have been designed to illustrate the comparison of the proposed intensity based metric to the average performance metric for linear and nonlinear cases. The results in this section seek to validate and explain in more detail the theoretical metrics comparison. Parameters $\alpha = 0.1$ and $\beta = 10$ are assumed constant in all cases. We used the linear recovery time function shown in Eq. 4.17 in all scenarios. In addition, in the nonlinear cases I is greater than one. Even though the values of the metric $R(I)$ are not bounded, they have been scaled between zero and one to ease the comparison with the average performance.

In the linear case the loss and recovery functions (see Eq. 4.16 and 4.17) have a linear structure based on the following form:

$$X = 0.1I \tag{4.16}$$

$$T = 10X \tag{4.17}$$

For the different scenarios the response variable functions are used to quantify $R(I)$ and $R(AP)$, the linear case is contrasted in the following figure.

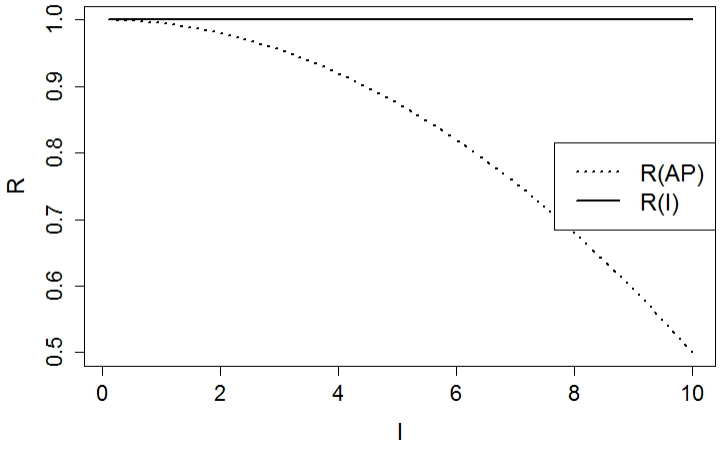

Figure 4.1: Resilience for linear absorptive and restorative capacities

From Fig. 4.1, the R(I) model shows a constant resilience at different levels of disruption intensity. This is because the absorptive and restorative capacities remain the same for increasing I. On the other hand, the average performance metric shows a quadratically decreasing resilience in response to increasing loss and recovery time for higher intensities. This is notwithstanding the fact that the system's response is commensurate with the increased values of intensity.

In the nonlinear cases we consider two groups of examples based on the response variables function shape. The first scenario is called high resilience sensitivity to I because the system resiliency decreases as the event magnitude increases. The second scenario is

defined as low resilience sensitivity to I, because the system resiliency increases as the event magnitude goes up. In the first group we discuss two examples: when X is based on Eq. 4.18 ($n > 1$) and when X has an exponential form (as in Eq. 4.19).

$$X = 0.1I^2 \tag{4.18}$$

$$X = 0.1e^I \tag{4.19}$$

Figures 4.2 and 4.3 respectively illustrate the two examples. In both cases, the two metrics show a decreasing resilience in response to increasing disruptive event intensity. However, while $R(AP)$ shows an increasing decline, the rate for $R(I)$ decreases, which captures the fact that the restorative capacity is able to remain constant while the performance loss X grows at an increasing rate.

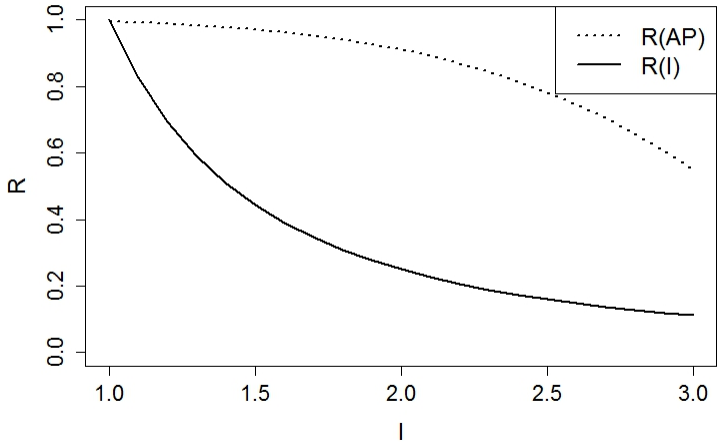

Figure 4.2: Resilience for nonlinear case ($n > 1$)

Despite some differences in the resilience drop rate explained above, both metrics describe a decreasing resilience pattern as I increases under the high sensitivity to I scenario. This is the only case where the metrics capture a equivalent behavior.

In the group for low resilience sensitivity to the event magnitude, we show two examples that mimic this scenario: the general nonlinear model for $0 < n < 1$ and the

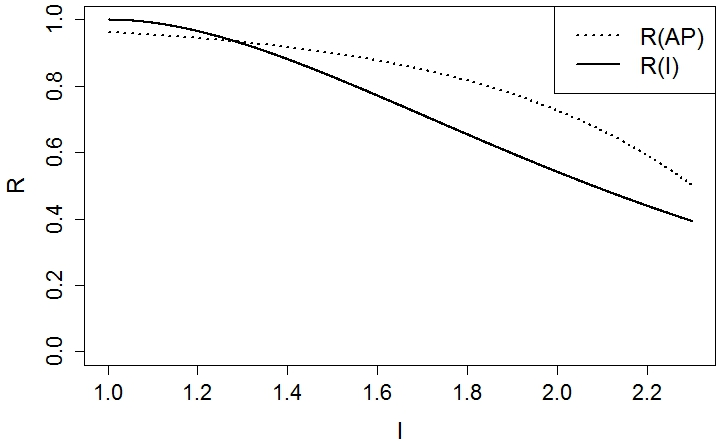

Figure 4.3: Resilience for an exponential absorptive capacity

logarithmic model with the following respective loss functions (Eq. 4.20 and 4.21). The first case, when we set the parameter $n = 0.3$ the absorptive capacity is given by the following nonlinear equation:

$$X = 0.1I^{0.3} \tag{4.20}$$

Then, the resulting figure 4.4 displays an increasing resilience system, which despite the loss and recovery time increments, the system ability to dissipate the event magnitude is improving.

A similar scenario is when the absorptive capacity follows a logarithmic shape provided by the next equation:

$$X = 0.1\ln(1 + I) \tag{4.21}$$

As expected, the $R(I)$ measurements from figures 4.4 and 4.5 show an increasing resilience as the marginal system response improves as I increases even though the total loss and recovery time get bigger. The average performance metric is unable to capture the improving response, thus showing a decreasing resilience trend. In this scenario and the linear case there are dissimilarities in the $R(I)$ and $R(AP)$ analysis, while the new

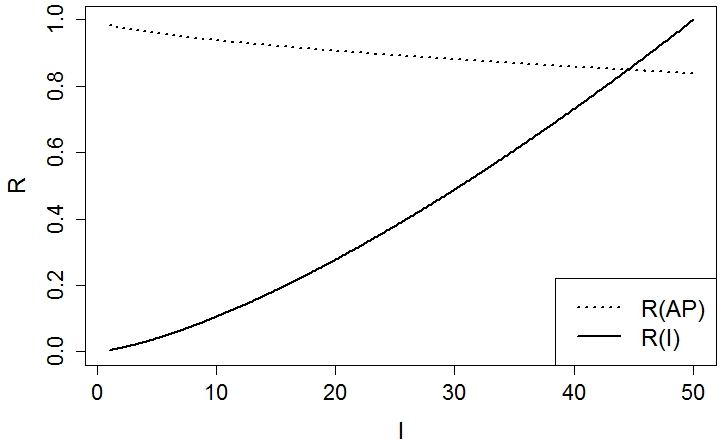

Figure 4.4: Resilience for nonlinear case ($0 < n < 1$)

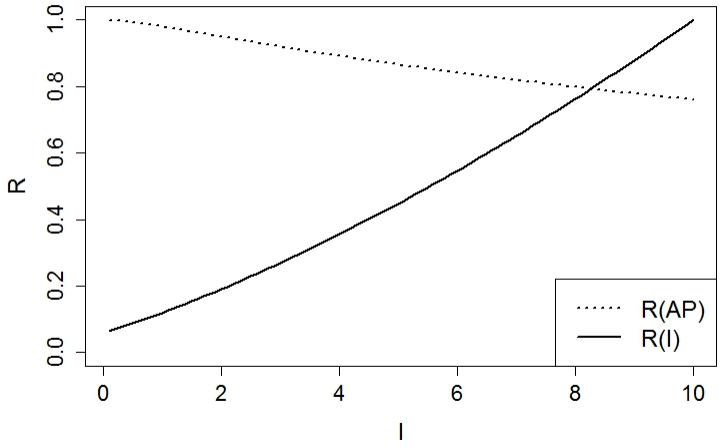

Figure 4.5: Resilience for a logarithmic absorptive capacity

metric models varying X, T and I relationships, the traditional metric can not capture these interactions.

The numerical analysis shows that the intensity based metric better captures different dynamics of the system response to varying disruption intensities whereas the average performance metric invariably shows a decreasing resilience.

4.3 Community Resilience Measurement After a Pandemic Outbreak

The pandemic outbreak testbed is based on the model [63] where an influenza virus is spread on a 1.5 million inhabitants community with the demographics of the USA . An agent based simulation model depicts the daily interactions in the community as people go to work, school or stay at home. As people begin the social mixing with infected individuals, then the higher is the probability to get transmitted the virus. An instance will stop once the community has recovered.

In the model, thirteen Mon Pharmaceutical Interventions (NPI) actions are deployed to evaluate their impact on community resilience. These strategies include quarantine days, isolation periods, isolation compliance, and number of infected people to close a school or workplace. The strategies are static, therefore the parameters are fixed from the beginning of every instance and will remain invariable until the next run.

The resilience analysis of a community impacted by a influenza pandemics is carried out in two sections. First, the new metric is compared with the average performance model to identify metrics differences on a baseline scenario without interventions and a recommended set of NPIs. Then, the significant NPI actions are established based on their impact in the maximum percentage of infected population and the community recovery time. Furthermore, this result is compared to the significant NPIs estimated based on the IAR metric.

The metric elements are the virus strength I, the response variables maximum loss of healthy population X and the recovery time T measured until the system has reached a 99% of healthy population. The metric comparison between $R(I)$ and $R(AP)$ is carried out for two scenarios: I) a baseline scenario with no interventions, II) NPI based on [63] .

Figures 4.6 and 4.7 show the relationship between the virus strength and the response variables. Both X and T are reduced when NPIs are implemented during the pandemic

outbreak. Consistently the NPI strategies improve the absorptive and restorative capabilities regardless the virus strength.

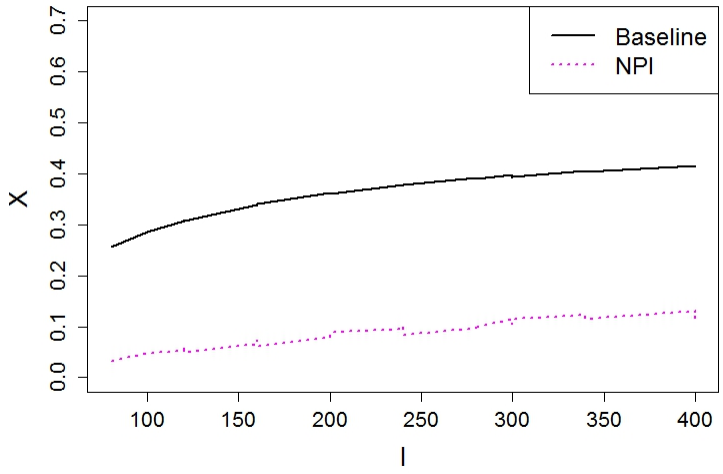

Figure 4.6: Maximum loss versus virus strength

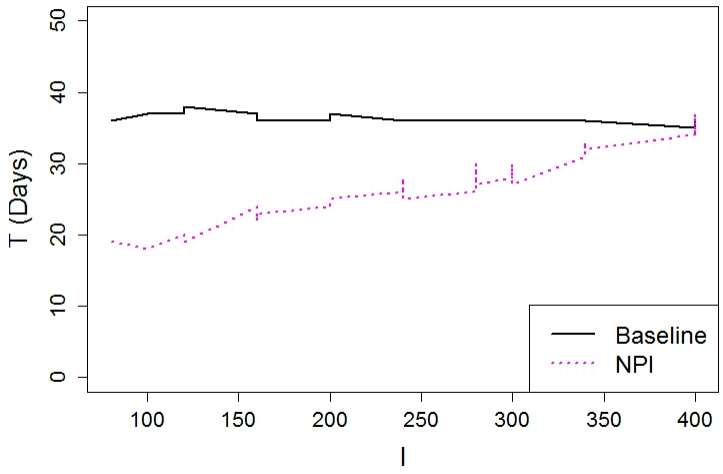

Figure 4.7: Recovery time versus virus strength

Once the response variables X and T have been assessed, community resilience is captured and compared by using the average performance and the new resilience metrics. Figures 4.8 and 4.9 display community resilience levels for varying virus strength.

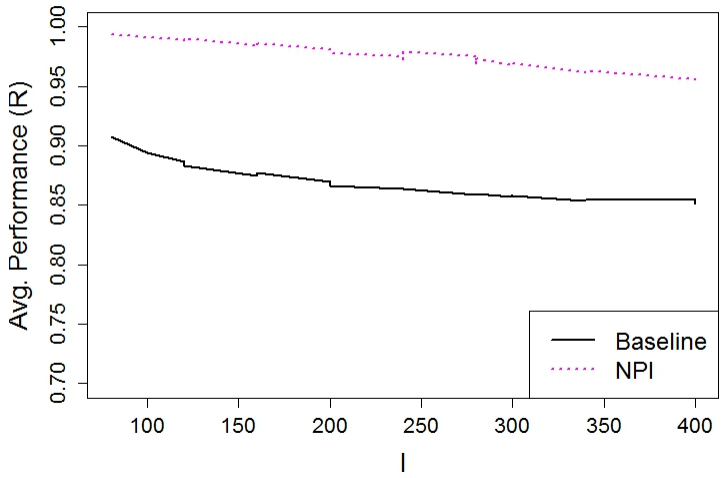

Figure 4.8: Average performance resilience metric

The average performance resilience metric invariably decreases as the virus strength increases. This behavior will repeat regardless the type of system, given that performance loss and recovery time are expected to increase as the disruption intensity grows. Thus, $R(AP)$ always suggests that systems ability to withstand and recover worsens when the disruption intensity goes up.

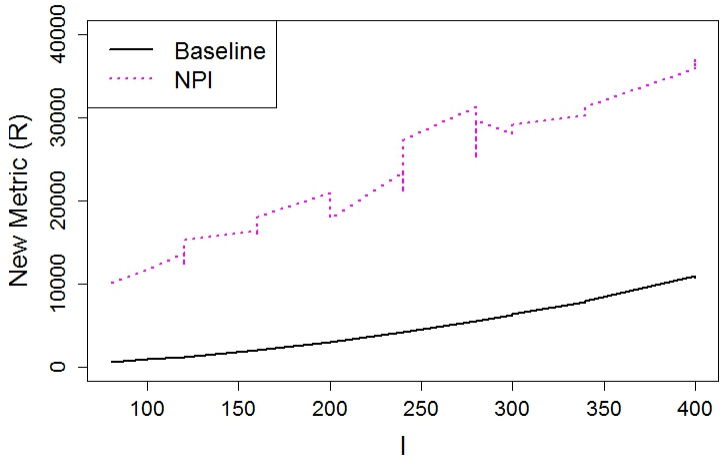

Figure 4.9: Intensity based resilience metric strategies comparison

In the case of the $R(I)$, resilience level improves as the virus strength increases. In the case study, community resilience is increasing despite that the performance loss and recovery time are worsening. This behavior is caused due to system ability to dissipate I per unit of the absorptive and restorative capacities. System resiliency is improving for the baseline and NPI scenarios as I increases, however the resilience gap between the scenarios gets higher as virus strength increases suggesting a increasingly increasing resilience.

Parameters changes in the NPIs affect system structure and resilience capacities which leads to varying resilience patterns. There are configurations where R(I) decreases or increases as the virus intensity gets stronger. Figure 4.10 depicts different strategies where the ability of the metric $R(I)$ to capture multiple resilience behaviors is highlighted as opposed to the ever decreasing pattern of the $R(AP)$.

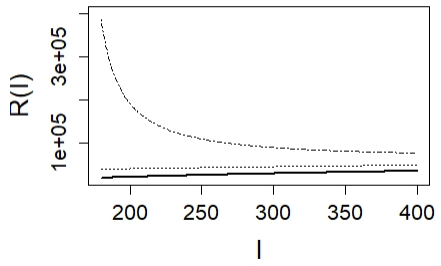

Figure 4.10: R(I) policies comparison

In general, an increasing resilience suggests a system that is getting stronger as the virus strength goes up. However, an interesting insight from Figure 4.10 is that an increasing resilience does not necessarily mean a better system than the one with a decreasing resilience pattern. Given the wide variety of policy configuration and resiliency profiles the next chapter identifies the interventions that maximize $R(I)$.

4.4 Supply Chain Resilience Measurement

Traditionally, supply chain resilience has been measured using qualitative tools based on surveys and experts opinions [53, 52]. In the few cases where resilience has been quantified using quantitative tools [59] implemented simulation models. Adopting the simulation approach, the supply chain resilience evaluation is carried out in a discrete model of a linear system with one node per echelon. The two echelon system serves a daily demand $N(100, 10)$ by using an (s, Q) inventory policy where Q units are reordered once the inventory position has decreased below the reorder point (s).

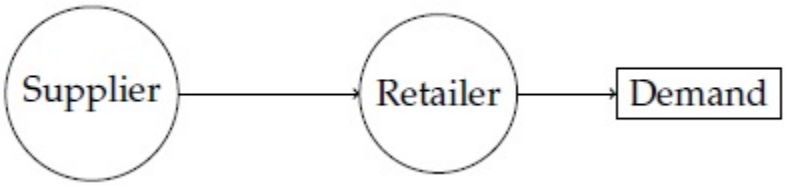

Figure 4.11: Supply chain configuration

The supply chain failure mode that was implemented in the model is the supplier disruption due to its relevance in the industry. This disruptive event will impede the physical flow through the supply chain from the supplier to the final customer. The event magnitude (I) is the supplier failure length which is assigned from a $unif(2, 30)$ days interval.The performance metric is the fraction of satisfied demand delivered on time. The simulation model was run for 365 days for multiple disruption intensity levels and the response variables were recorded for each replication. The performance loss metric X refers to the maximum percentage unsatisfied demand, and the recovery time T was measured from the time that the disruption affected the service level (less than 95 %) until the system performance was restored to the initial state.

The response variable X from figure 4.12 is less than 100 % for small disruptions but as I increases the system goes from a partial to a complete unsatisfied demand, wich means

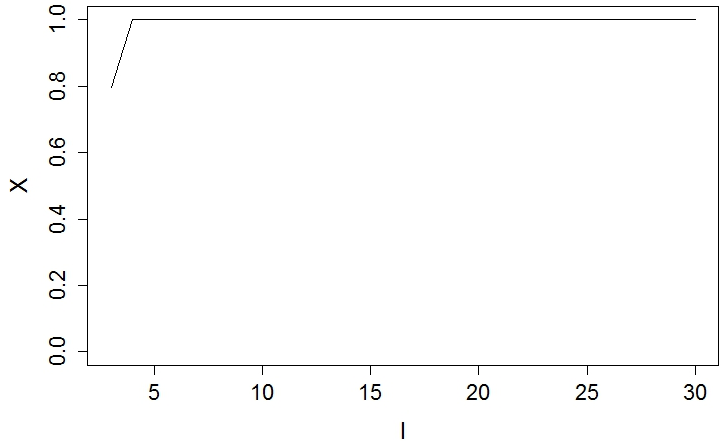

Figure 4.12: Supply chain performance loss

that the loss is 100 %. The absorptive capacity as a rate of X and I increases once the maximum loss is 100 %.

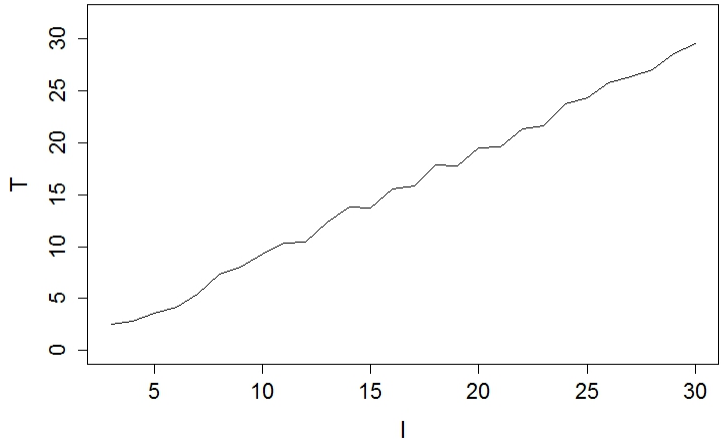

Figure 4.13: Supply chain recovery time

In figure 4.13 the recovery time is directly proportional to the supplier disruption time. The highest values of the recovery time relative to I are for small disruptions.

The resilience comparison from figure 4.14 shows that in the case of $R(AP)$ the resilience decreases which is the behavior that is always described by this metric. On the other hand, the new metric $R(I)$ describes an increasing resilience. This behavior can be

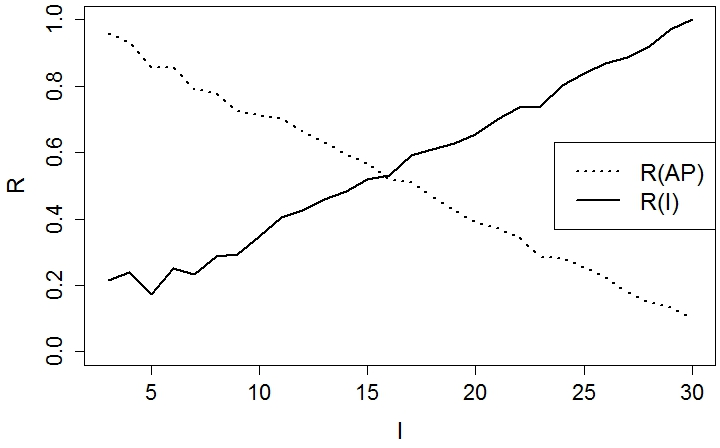

Figure 4.14: Supply chain resilience metrics comparison

explained by the pattern of both response variables X and T. The absorptive capacity improves because the performance loss remains equal to 1 for medium and high intensity disruptions. In addition, the recovery time is higher than the supplier disruption for small intensity events, but for medium and large disruptions T and I are approximately the same, leading to an increasing resilience.

In this chapter R(I) displayed a higher flexibility to capture accurately diverse resilience patterns, such as constant, increasing and decreasing resilience. The application in social and physical systems confirm the importance of measuring resilience as a function of I to avoid the invariable decreasing pattern captured by the average performance metric.

5 RESILIENCE DRIVERS ESTIMATION

The previous chapters explored a new metric to measure supply chain and community resilience. In this chapter the analysis is extended to the identification of resilience drivers in the physical and social systems under study.

5.1 Community Resilience Driver Estimation

Resilience drivers in the studied social system are identified using the response variables X and T. All the analyses in this section are intended to increase system resilience by improving both capacities. The policies cost was not included in this research.

A total of 128 scenarios are evaluated based on Cohen's power analysis with $\alpha = 0.05$ and $\beta = 0.1$. The parameter values for every NPI are taken from the ranges used in [63]. Table 5.1 displays the parameters generator functions for each scenario. Once the parameters are generated for a single run, the values are not changed.

A first analysis is performed using a linear regression with the IAR as the response variable with an R^2 of 0.87. The NPIs that are significant in the analysis are the cases to close a class, classes to close a school and class quarantine period. In this approach it is not determined how these NPIs will affect the absorptive and restorative capacities separately.

An independent evaluation is carried out using linear regression models to both dependent variables. The maximum percentage of infected population and the recovery time from the pandemic outbreak yield an R^2 of 0.89 and 0.87, respectively. The common significant factors for both variables are virus strength, cases to close a class, and number

Table 5.1: NPIs generator parameters

NPI	Parameters
Delay days quarantine	Unif(3,7)
Isolation period	Unif(7,10)
Isolation compliance workers	Unif(0.53,0.75)
Isolation compliance non-workers	Unif(0.57,0.84)
Household quarantine period	Unif(7,10)
Household compliance workers	Unif(0.53,0.75)
Household compliance non-workers	Unif(0.57,0.84)
Cases to close a class	Unif(1,3)
Classes to close a school	Unif(1,3)
School clousure duration	Unif(21,42)
Cases to close mixing groups workplaces	Unif(3,5)
% mixing groups to close workplaces	Unif(0.3,0.5)
Mixing group quarantine period	Unif(7,14)

of classes to close a school. The NPI cases to close mixing groups workplaces has incidence on T. Under this approach the effects of the NPIs on the response variables are known. From table 5.2 it is observed that there is a positive relationship among the rel-

Table 5.2: Linear regression coefficients based on response variables X and T

Factor	**Coefficients**	
	X	T
I	0.00031	0.04625
Cases to close a class	0.05543	2.06824
Classes to close a school	0.03497	1.08036
Cases to close mixing groups workplaces	NA	1.67599

evant NPIs and the response variables, thus the best performance will be reached when the minimum values are implemented for the significant NPIs. This approach suggests a highly sensitive triggers policy where schools and workplaces will shut down once few infected cases have been detected.

The resilience analysis using two response variables is contrasted with the results obtained by using the IAR as the desired metric to be minimized. Based on the same number of observations, the significant NPIs found are not the same. In the case of the response

variables X and T, besides the school related NPIs, the cases to close mixing groups at work is a significant intervention. The benefit of the resilience analysis over the traditional IAR is that policy makers and authorities are getting more specific information about how the interventions are impacting the absorptive and restorative capacities.

The importance of school related NPIs in both analysis is confirmed by a disaggregated study of the infected population per age group 0-19,20-64, and 65-99 years old. Figure 5.1 evidences that the maximum relative percentage of infected population is at ages 0-19. An statistical analysis is performed using an ANOVA and pairwise mean comparison that confirms that results are consistent for both response variables X and T. The

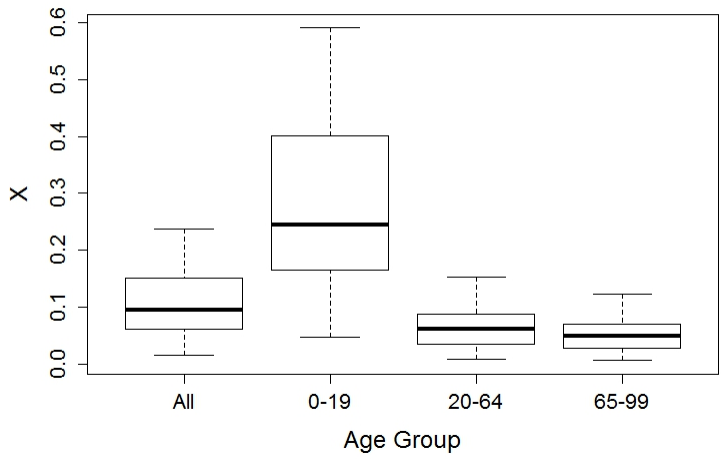

Figure 5.1: Age groups comparison dependent variable X

resilience analysis points out the importance of NPIs targeting the age group between 0-19 years. Both dependent variables will benefit from highly sensitive course and schools closure trigger points, which increase system resilience levels.

The case study in this section confirmed the importance of an intensity based resilience metric in social systems given that it was able to capture more complex system response relationships as opposed to the average performance metric. Furthermore, the regression analysis of both dependent variables enables decision makers to mobilize resources to improve specific resilience capacities.

5.2 Supply Chain Resilience Driver Estimation

Supply chain resilience drivers have been discussed in a strategic fashion without the proper modeling of operational policies and their impact on system resiliency. Drivers such as redundancy, network design, and collaboration are recurrently mentioned as resilience drivers. In this section the redundancy and network structure strategies are operationalized by analyzing the supplier location, order size, and safety stock.

Table 5.3: Supply chain strategies and policies

Parameters	Value
Supplier Disruption	Unif(2,30)
Order Size	Unif(2,15)
Lead Time	Unif(1,7)
Safety Stock	Unif(0.5,0.999)

Table 5.3 displays the values for the network parameters. The order size is measured as the number of average demand days. The lead time is the replenishment time, and the safety is the service level based on demand uncertainty during a restock cycle.

A regression analysis is carried out to identify the supply chain resilience drivers based on the maximum performance loss and the recovery time response variables with R^2 values of 0.62 and 0.94 respectively.

Table 5.4: Supply chain regression coefficients based on response variables X and T

Factor	**Coefficients**	
	X	T
Supplier Disruption	0.00930	0.97398
Order Size	-0.0098	-0.7889
Lead Time	NA	0.43836
Safety Stock	-0.1707	NA

From table 5.4 the supply chain absorptive capacity or static resilience improves when either the order size or the safety stock increase. The restorative capacity improves when either the order size increases or the lead time decreases. These results are valid for the given configuration and supplier disruption failure mode. In general, the studied model

will improve resiliency levels for suppliers disruptions by decreasing lead times, and increasing order size and safety stock.

The analysis in the supply chain highlights the importance of quantifying the relationship of system structure and policies with resilience related response variables. While these results can not be generalized from a single example it sets a standard on capturing these relationships.

6 RESILIENCE OPTIMIZATION MODELS

This chapter proposes static resource allocation models to maximize resilience capacities. While traditional models maximize resilience by using a single metric, the suggested approach gives the same importance to resilience dimensions. A multi-objective model is used to improve systems resiliency in numerical examples and the social system previously defined in this report.

6.1 Multi-Objective Resilience Optimization

Two bi-objective budget allocation models are presented to optimize system absorptive and restorative capacities. The first dimension, refers to the ability to withstand a disruption and it is measured as the maximum performance loss [16]. Resource allocation towards this capability requires hardening strategies, such as redundancy [80] and fortification [81].The second dimension is the ability to restore system performance after a disruptive event. This property is measured as the recovery time [8]. The actions to improve this property will increase system speed to return to the initial or desired state.

The proposed models to optimize these two key dimensions are a bi-objective linear program and a bi-objective mixed integer program (MIP). In both cases a comparative analysis is carried out with the single objective counterpart based on [20] formulation.

6.1.1 Bi-objective Linear Program

In these formulations a linear resource allocation is assumed for both response variables and the final outcome is the recommended investment in the absorptive and restora-

tive capacities. The notation for the single objective and multi-objective formulations have the following decision variables:

z_x investment to harden the system

z_t investment to increase recovery capability

The model parameters are listed as follow:

X' maximum performance loss without investment

T' recovery time without investment

α performance improvement per unit of investment

β Recovery time improvement per unit of investment

The single objective formulation is a Non Linear Program (NLP) that maximizes resilience based on a linear approximation of the widely used average performance metric, originally proposed by [12] and further implemented by many authors [78, 30].

$$\max 1 - \frac{(X' - \alpha z_x)(T' - \beta z_t)}{2 * T_{\max}} \tag{6.1}$$

$$\text{s.t. } \gamma x + \tau t \leq B \tag{6.2}$$

$$\alpha x \leq X^{'} \tag{6.3}$$

$$\beta t \leq T^{'} \tag{6.4}$$

In this model, when linear or exponential allocations functions are assumed then the optimal solutions are to invest the available budget in a single resilience dimension, either to decrease X' or T' [20]. The main drawback of these solutions is that from a practical perspective the investment of the whole budget in a single capacity will affect the improvement of other resilience capacity. A more balanced approach should be considered before making a final decision.

In the case of the bi-objective formulation, since decision variables are continuous and all of the equations are linear, then this model has lower complexity than the nonlinear single objective counterpart, where the multiplication of the objectives X and T develops

a nonlinear structure that arises higher complexity. The next formulation capture liner continuous allocation for both resilience capacities:

$$\min X' - \alpha z_x \tag{6.5}$$

$$\min T' - \beta z_t \tag{6.6}$$

$$\text{s.t}\, z_x + z_t \leq B \tag{6.7}$$

$$\alpha z_x \leq X' \tag{6.8}$$

$$\beta z_t \leq T' \tag{6.9}$$

The objective functions (6.5) and (6.6) minimize the initial loss and recovery time. The budget constrain (6.7) limits the allocation capacity, and constrains (6.8) and (6.9) are the maximum reductions of X' and T'. The main benefits of this formulation are the lower structure complexity and that it can provide multiple non-dominated solutions given the Pareto front that is derived in multi-objective problems.

The solutions found in the single objective resilience model for the linear and exponential allocation are included in the corner points of the bi-objective Pareto front given that these are non-dominated solutions. The fact that the milti-objective model solutions include the single objective model solution gives an edge to our approach because more well balanced options are available to decision makers.

6.1.2 Bi-objective MIP Formulation

The Mixed Integer Program (MIP) models enable resource allocation of specific hardening and recovery strategies, in contrast with the previous models where individual strategies were not available. The assumption of a set of strategies that can improve one or two dimension simultaneously fits real life settings where decision makers will choose from the available options a subset of alternatives instead of using a continuous allocation function. The linear continuos functions capture the system improvement per unit

of money invested. Even though these models may fit better real settings, the main limitation is their complexity when contrasted with the linear models. The notation of these formulations have the following decision variables:

z_i: Binary variable indicating whether or not action i is selected

The models parameters are as follow:

X' Maximum performance loss without investment

T' Recovery time without investment

α_i Strategy i performance improvement

β_i Strategy i Recovery time improvement

The single objective model is a mixed integer nonlinear program (MINLP). The complexity of these models has been less studied due to the lack of general structure [82]. This model has the same constraints than the single objective NLP.

$$\max 1 - \frac{(X' - \sum_{i=1}^{n} \alpha_i z_i)(T - \sum_{i=1}^{n} \beta_i z_i)}{2 * T_{max}} \tag{6.10}$$

$$\text{s.t} \sum_{i=1}^{n} c_i z_i \leq B \tag{6.11}$$

$$\sum_{i=1}^{n} \alpha_i z_i \leq X' \tag{6.12}$$

$$\sum_{i=1}^{m} \beta_i z_i \leq T' \tag{6.13}$$

Although the bi-objective MIP is NP-hard its structure has been revised and more algorithms are available to obtain near optimal solutions in contrast with the MINLP.

$$\min X' - \sum_{i=1}^{n} \alpha_i z_i \tag{6.14}$$

$$\min T' - \sum_{i=1}^{n} \beta_i z_i \tag{6.15}$$

$$\text{s.t} \sum_{i=1}^{n} c_i z_i \leq B \tag{6.16}$$

$$\sum_{i=1}^{n} \alpha_i z_i \leq X' \tag{6.17}$$

$$\sum_{i=1}^{n} \beta_i z_i \leq T' \tag{6.18}$$

The objective functions minimize the maximum loss and the recovery time by selecting the optimal subset of hardening and recovery strategies. For a single strategy i at least one of the coefficients α_i or β_i should be greater than zero, otherwise the alternative will be discarded. The model allows the possibilities that one strategy may improve both resilience capabilities, and that by increasing on capacity the other may be reduced.

Among the benefits of the proposed multi-objective models the most significant are the multiple non-dominated solutions and flexibility to include multiple hardening and recovery actions while keeping less complex model structures.

6.1.3 Strategies Selection

Once the models have been solved, in the case of the single objective most of the times a unique alternative will be found, while in the multi-objective model a Pareto front with a variety of non-dominated alternatives will be available. Therefore, two approaches are suggested to select the most suitable resource allocation based on the decision makers preferences.

The first method, which is based on the idea of maximizing resilience, is to compute a subset of resilience metrics $\{R_1, R2..., Rm\}$, and then based on a voting system or a combined metric choose the best allocation strategy.

The second method is to implement the common tools to point selection in the multi-objective analysis field. This includes either minimize the measurement of the normalized euclidean distance from the ideal point to the Pareto front, or maximize the distance between the non-dominated solutions and the Nadir point.

6.1.4 Illustrative Example: Bi-objective LP

A numerical example is developed to illustrate the bi-objective resilience optimization analysis for the LP model. The parameter generation rules are summarized in table 6.1.

Table 6.1: MO LP example parameters

Parameter	MO- LP
X'	$unif(0.2, 1)$
T'	$unif(10, 100)$
α	$unif(0.001, 0.5)$
β	$unif(0.005, 1)$
B	$min(\frac{X'}{\alpha}, \frac{T'}{\beta})$
c_i	NA

The evaluation of the Bi-objective LP model is performed over 1000 instances. It is assumed that the available budget can not fully restored X' and T'. Then the bi-objective LP model is easily solved by identifying all the allocation strategies where B is completely spent in z_x and z_T.

The Pareto front in Figure 6.1 depicts a general representation of the non-dominated points in the line where the corner points are $(X' - \alpha * B, T')$ and $(X', T' - \beta * B)$. Once the non-dominated solutions are identified for each instance the next step is to select the best possible point.

The first method deploys three resilience metrics R_1 [16], R_2 [15] and the intensity based resilience metric R_3. The following parameters are elements of these metrics. T^* is

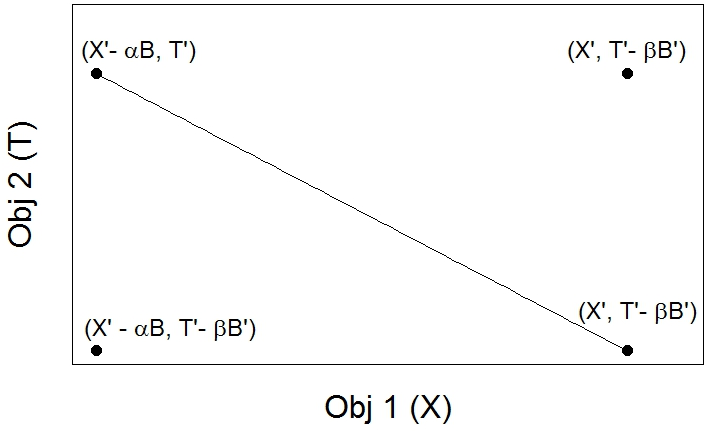

Figure 6.1: Pareto front multi-objective LP

the control or maximum time , S_p is the speed recovery factor, F_0 is the initial performance level, F_d is the performance when the system is disrupted, F_r is the performance level when the system is stable after recovery, and I is the disruptive event magnitude.

$$R_1 = 1 - \frac{XT}{2T^*} \tag{6.19}$$

$$R_2 = S_p \frac{F_r}{F_0} \frac{F_d}{F_0} \tag{6.20}$$

$$R_3 = \frac{I^2}{XT} \tag{6.21}$$

In 99% of the evaluated instances there is an agreement among the three metrics in the selection of the best non-dominated point. The chosen points where located in the Pareto front corners, this happened in 100% of the instances for R_1 and R_2, and 99.6% of the times in R_3.

Method 2 is based on the estimation of the normalized euclidean distance. In contrast with method 1, 100% of the selected points are not corner points in the Pareto front. Therefore, it is confirmed that the single resilience metrics will favor corner points, while the euclidean distance approach finds a balance between the resilience capabilities.

6.2 Pandemic Outbreak Resilience Optimization

In the community resilience analysis the response variables X and T were fitted in chapter 5, as result the significant variables are related to schools and workplaces.

I: Virus strength

X_1: Cases to quarantine mixing groups at schools

X_2: Mixing groups to close schools

X_3: Cases to quarantine mixing groups at workplaces

$$\min X \; -0.1345 + 0.0000297I + 0.0513X_1 + 0.0339X_2 \tag{6.22}$$

$$\min T \; 2.1968 + 0.0459I + 2.2709X_1 + 1.3118X_2 + 1.734X_3 \tag{6.23}$$

When the objectives (6.22) and (6.23) are analyzed the unique non dominated point is when the three strategies are implemented with the minimum possible values which are $X_1 = 1$, $X_2 = 1$ and $X_3 = 3$. This point minimizes X and T, hence it maximizes resilience. This policy will improve the resiliency levels because it will shut down schools with infected individuals faster, reducing the number of interactions between infected and healthy students.

Even though the non-pharmaceutical interventions benefit the response variables, this policy has a social impact in the students and workers missing classes and work. Two new objectives are added to account for this impact, the total number of student days without school and the worker days without work.

$$\min Students \; 100297065 + 56078I - 18865869X_1 - 12646872X_2 + 2212280X_3 \tag{6.24}$$

$$\min Workers \quad Days \; 498708.6 + 2144.1I + 129626.2X_1 + 20678X_2 - 179114X_3 \tag{6.25}$$

The selected NPIs have significance in the objectives (6.24) and (6.25) with R^2 values 0.8548 and 0.642 respectively. Then the four objectives are included in the analysis to improve resilience and mitigate the social impact on students and workers. The evaluation is performed in the different objectives subsets in order to identify better balanced policies. The minimum distance from the best combination of X, T and the students days

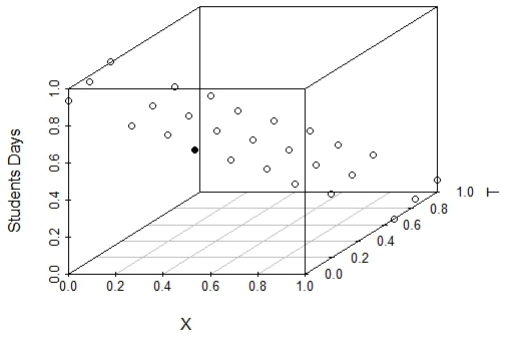

Figure 6.2: NPIs impact on students days, X and T

without classes to the best performance of the individual objectives is the black solid point in figure 6.2 which corresponds to the policy $X_1 = 1$, $X_2 = 3$ and $X_3 = 3$. This strategy provide the best balance of the three objectives.

The minimum distance from the best combination of X, T and the total workers days

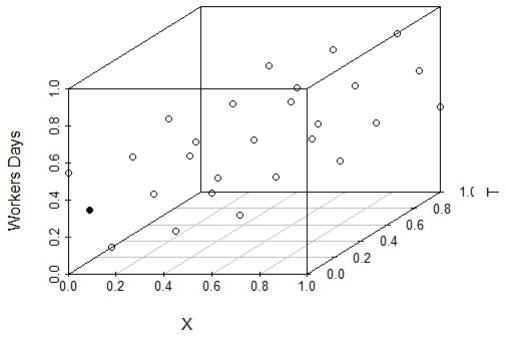

Figure 6.3: NPIs impact on workers days, X and T

off to the possible strategies is the black solid point in figure 6.2 which corresponds to the policy $X_1 = 1$, $X_2 = 1$ and $X_3 = 4$. Table 6.2 displays the best strategies to improve indi-

Table 6.2: NPI strategies and objectives result

X_1	X_2	X_3	Result
1	1	3	Optimize R, X and T
3	3	3	Minimize total days of students without class
1	1	5	Minimize total days of workers without work
1	3	3	Best balance of X, T and Students days
1	1	4	Best balance of X, T and Workers days
1	3	4	Best balance of the four objectives

vidual objectives and bundles where two, three and four objectives are balanced. Similar metrics or a cost based combination can be added to account for additional social factors or to represent decision makers interests.

The benefits of multi-objective model are the linearity and flexibility to incorporate multiple dimensions of system resilience. This approach provides a generalization in the resilience analysis where multiple resilience metrics can be implemented to select a strategy to improve resiliency.

7 CONCLUSION

Accurate resilience estimation enables decision makers to improve system absorptive and restorative capabilities. Previous works have suggested the importance of the disruption intensity in a multi-dimensional resilience analysis. Our model is the first formal approach that explicitly incorporates the intensity dimension in a resilience metric.

The proposed model can properly capture linear and nonlinear relationships among performance loss, recovery time, and disruption intensity. The new metric was compared to the average performance metric analytically, through numerical illustrative examples, and case studies. The results suggest that the intensity based model provides a better estimation of resilience, mainly in the cases when a system's response is commensurate or improving with increased disruption intensities.

In addition, the new metric is independent of the "control time" or maximum time (T^*) parameter(s) present in the average performance models. The elimination of these subjective parameters improves the application and comparison within and across resilience driven system designs.

The identification of the structure, policies, and operational variables improve systems ability to absorb and recover from a disruptive event is a key element to improve system resiliency. Two tests beds were evaluated, a social and a physical system.

In the social system, a community resilience assessment enriches the traditional Infection Attack Rate analysis by combining the absorptive and restorative capacities, and enabling the addition of other factors considering the multi dimensional nature of the resilience concept.

The Resilience drivers identification in a community affected by a pandemic outbreak showed the importance of evaluating the resilience capabilities X and T, because decision makers are given more information about how each significant intervention will improve community response. This approach leads to a targeted resilience improvement as opposed to the IAR metric that aggregates the interventions towards a single index. As a result, resilience level is higher when the NPIs were chosen to improve the absorptive and restorative capacities.

In the physical test, the supply chain analysis identified the order size, lead time and safety stock service level as key variables to manage resilience levels. This study contributes the measurement of the relationship between operational variables and supply chain resilience.

The drivers estimation is used to define the best path to allocate resources towards resilience improvement. A multi-objective model is suggested for LP and MIP structures to optimize systems ability to absorb and restore after a failure. The contribution of this approach is the flexibility to include addition resilience capabilities without sacrificing the linear complexity. Following this analysis, community resilience strategies to face pandemic influenza outbreaks were identified while balancing absorptive capacity, restorative capacity, and social impact.

7.1 Future Research

Future extensions of this research are divided in three categories: metrics, applications, and resource allocation. In the first category, it is expected to seek the development of time dependent metrics to perform (near) real-time resilience analysis and online decision support based on resilience improvement. While the proposed metric included two resilience dimensions, it should be open to include more key capabilities such as the adaptive capacity. Another limitation of the current model is the assumption of determin-

istic parameters, particularly, the disruption intensity. We will work to develop stochastic, time dependent resilience metrics to provide more accurate resiliency estimation.

In the second category, research will focus on three aspects to enhance community and supply chain resilience: i) New applications in social systems with the intention to test R(I) in areas other than public health. ii) Explore quantitative metrics and drivers to include the adaptive capacity in the resilience analysis. Even though this capacity is included consistently in social systems it is not frequently measured. iii) Evaluate additional supply chain resilience drivers such as collaboration, network structure and flexibility.

In the third category, we expect to develop dynamic resource allocation to improve system resilience based on the independent resilience capacities. Furthermore, uncertainty in parameters will be tackled using robust optimization.

REFERENCES

[1] S. L. Cutter, "The landscape of disaster resilience indicators in the usa," *Natural Hazards*, vol. 80, no. 2, pp. 741–758, 2016.

[2] R. J. Klein, R. J. Nicholls, and F. Thomalla, "Resilience to natural hazards: How useful is this concept?," *Global Environmental Change Part B: Environmental Hazards*, vol. 5, no. 1, pp. 35–45, 2003.

[3] R. Bhamra, S. Dani, and K. Burnard, "Resilience: the concept, a literature review and future directions," *International Journal of Production Research*, vol. 49, no. 18, pp. 5375–5393, 2011.

[4] S. Hosseini, K. Barker, and J. E. Ramirez-Marquez, "A review of definitions and measures of system resilience," *Reliability Engineering & System Safety*, vol. 145, pp. 47–61, 2016.

[5] R. Pant, K. Barker, J. E. Ramirez-Marquez, and C. M. Rocco, "Stochastic measures of resilience and their application to container terminals," *Computers & Industrial Engineering*, vol. 70, pp. 183–194, 2014.

[6] S. L. Cutter, L. Barnes, M. Berry, C. Burton, E. Evans, E. Tate, and J. Webb, "A place-based model for understanding community resilience to natural disasters," *Global environmental change*, vol. 18, no. 4, pp. 598–606, 2008.

[7] G. Windle, "What is resilience? a review and concept analysis," *Reviews in Clinical Gerontology*, vol. 21, no. 2, pp. 152–169, 2011.

[8] G. P. Cimellaro, A. M. Reinhorn, and M. Bruneau, "Framework for analytical quantification of disaster resilience," *Engineering Structures*, vol. 32, no. 11, pp. 3639–3649, 2010.

[9] I. Linkov, D. A. Eisenberg, K. Plourde, T. P. Seager, J. Allen, and A. Kott, "Resilience metrics for cyber systems," *Environment Systems and Decisions*, vol. 33, no. 4, pp. 471–476, 2013.

[10] R. Pant, K. Barker, and C. W. Zobel, "Static and dynamic metrics of economic resilience for interdependent infrastructure and industry sectors," *Reliability Engineering & System Safety*, vol. 125, pp. 92–102, 2014.

[11] M. Ouyang and Z. Wang, "Resilience assessment of interdependent infrastructure systems: With a focus on joint restoration modeling and analysis," *Reliability Engineering & System Safety*, vol. 141, pp. 74–82, 2015.

[12] M. Bruneau, S. E. Chang, R. T. Eguchi, G. C. Lee, T. D. O'Rourke, A. M. Reinhorn, M. Shinozuka, K. Tierney, W. A. Wallace, and D. von Winterfeldt, "A framework to quantitatively assess and enhance the seismic resilience of communities," *Earthquake spectra*, vol. 19, no. 4, pp. 733–752, 2003.

[13] S. E. Chang and M. Shinozuka, "Measuring improvements in the disaster resilience of communities," *Earthquake Spectra*, vol. 20, no. 3, pp. 739–755, 2004.

[14] D. Henry and J. E. Ramirez-Marquez, "Generic metrics and quantitative approaches for system resilience as a function of time," *Reliability Engineering & System Safety*, vol. 99, pp. 114–122, 2012.

[15] R. Francis and B. Bekera, "A metric and frameworks for resilience analysis of engineered and infrastructure systems," *Reliability Engineering & System Safety*, vol. 121, pp. 90–103, 2014.

[16] C. W. Zobel, "Representing perceived tradeoffs in defining disaster resilience," *Decision Support Systems*, vol. 50, no. 2, pp. 394–403, 2011.

[17] G. Windle, K. M. Bennett, and J. Noyes, "A methodological review of resilience measurement scales," *Health and quality of life outcomes*, vol. 9, no. 1, p. 8, 2011.

[18] N. A. Marshall, "Understanding social resilience to climate variability in primary enterprises and industries," *Global Environmental Change*, vol. 20, no. 1, pp. 36–43, 2010.

[19] A. Plough, J. E. Fielding, A. Chandra, M. Williams, D. Eisenman, K. B. Wells, G. Y. Law, S. Fogleman, and A. Magaña, "Building community disaster resilience: perspectives from a large urban county department of public health," *American Journal of Public Health*, vol. 103, no. 7, pp. 1190–1197, 2013.

[20] C. A. Mackenzie, H. Baroud, and K. Barker, "Static and dynamic resource allocation models for recovery of interdependent systems: application to the Deepwater Horizon oil spill," *Annals of Operations Research*, vol. 236, no. 1, pp. 103–129, 2016.

[21] Y. Wang, C. Chen, J. Wang, and R. Baldick, "Research on Resilience of Power Systems Under Natural Disasters:A Review," *IEEE Transactions on Power Systems*, vol. 31, no. 2, pp. 1–10, 2015.

[22] W. Yuan, J. Wang, F. Qiu, C. Chen, C. Kang, and B. Zeng, "Robust optimization-based resilient distribution network planning against natural disasters," *IEEE Transactions on Smart Grid*, vol. 7, no. 6, pp. 2817–2826, 2016.

[23] G. Galindo and R. Batta, "Prepositioning of supplies in preparation for a hurricane under potential destruction of prepositioned supplies," *Socio-Economic Planning Sciences*, vol. 47, no. 1, pp. 20–37, 2013.

[24] N. Kunz, G. Reiner, and S. Gold, "Investing in disaster management capabilities versus pre-positioning inventory: A new approach to disaster preparedness," *International Journal of Production Economics*, vol. 157, no. 1, pp. 261–272, 2014.

[25] C. G. Rawls and M. A. Turnquist, "Pre-positioning of emergency supplies for disaster response," *Transportation Research Part B: Methodological*, vol. 44, no. 4, pp. 521–534, 2010.

[26] T. Young and P. Kelland, *A Course of Lectures on Natural Philosophy and the Mechanical Arts: pt. I. Mechanics. pt. II. Hydrodynamics. pt. III. Physics*, vol. 1. Taylor and Walton, 1845.

[27] C. S. Holling, "Resilience and stability of ecological systems," *Annual review of ecology and systematics*, pp. 1–23, 1973.

[28] S. Carpenter, B. Walker, J. M. Anderies, and N. Abel, "From metaphor to measurement: resilience of what to what?," *Ecosystems*, vol. 4, no. 8, pp. 765–781, 2001.

[29] A. Rose, "Defining and measuring economic resilience to disasters," *Disaster Prevention and Management: An International Journal*, vol. 13, no. 4, pp. 307–314, 2004.

[30] B. M. Ayyub, "Systems resilience for multihazard environments: Definition, metrics, and valuation for decision making," *Risk Analysis*, vol. 34, no. 2, pp. 340–355, 2014.

[31] C. W. Zobel and L. Khansa, "Characterizing multi-event disaster resilience," *Computers & Operations Research*, vol. 42, pp. 83–94, 2014.

[32] C. W. Zobel and L. Khansa, "Quantifying cyberinfrastructure resilience against multi-event attacks," *Decision Sciences*, vol. 43, no. 4, pp. 687–710, 2012.

[33] D. A. Reed, K. C. Kapur, and R. D. Christie, "Methodology for assessing the resilience of networked infrastructure," *IEEE SYSTEMS JOURNAL*, vol. 3, no. 2, 2009.

[34] C. A. MacKenzie and C. W. Zobel, "Allocating resources to enhance resilience, with application to superstorm sandy and an electric utility," *Risk Analysis*, 2015.

[35] E. Miller-Hooks, X. Zhang, and R. Faturechi, "Measuring and maximizing resilience of freight transportation networks," *Computers & Operations Research*, vol. 39, no. 7, pp. 1633–1643, 2012.

[36] M. Janić, "Modelling the resilience, friability and costs of an air transport network affected by a large-scale disruptive event," *Transportation Research Part A: Policy and Practice*, vol. 71, pp. 1–16, 2015.

[37] A. Asadzadeh, T. Kötter, and E. Zebardast, "An augmented approach for measurement of disaster resilience using connective factor analysis and analytic network process (fâĂŹanp) model," *International Journal of Disaster Risk Reduction*, vol. 14, pp. 504–518, 2015.

[38] S. L. Cutter, C. G. Burton, and C. T. Emrich, "Disaster resilience indicators for benchmarking baseline conditions," *Journal of Homeland Security and Emergency Management*, vol. 7, no. 1, 2010.

[39] H. Baroud, J. E. Ramirez-Marquez, K. Barker, and C. M. Rocco, "Stochastic measures of network resilience: Applications to waterway commodity flows," *Risk Analysis*, vol. 34, no. 7, pp. 1317–1335, 2014.

[40] C. Rougé, J.-D. Mathias, and G. Deffuant, "Extending the viability theory framework of resilience to uncertain dynamics, and application to lake eutrophication," *Ecological indicators*, vol. 29, pp. 420–433, 2013.

[41] B. D. Youn, C. Hu, and P. Wang, "Resilience-driven system design of complex engineered systems," *Journal of Mechanical Design*, vol. 133, no. 10, p. 101011, 2011.

[42] Z. Hu and S. Mahadevan, "Resilience assessment based on time-dependent system reliability analysis," *Journal of Mechanical Design*, vol. 138, no. 11, p. 111404, 2016.

[43] S. Hosseini, N. Yodo, and P. Wang, "Resilience modeling and quantification for design of complex engineered systems using bayesian networks," in *ASME 2014 International Design Engineering Technical Conferences and Computers and Information in Engineering Conference*, pp. V02AT03A040–V02AT03A040, American Society of Mechanical Engineers, 2014.

[44] N. Yodo and P. Wang, "Resilience modeling and quantification for engineered systems using bayesian networks," *Journal of Mechanical Design*, vol. 138, no. 3, p. 031404, 2016.

[45] K. Magis, "Community resilience: An indicator of social sustainability," *Society and Natural Resources*, vol. 23, no. 5, pp. 401–416, 2010.

[46] F. H. Norris, S. P. Stevens, B. Pfefferbaum, K. F. Wyche, and R. L. Pfefferbaum, "Community resilience as a metaphor, theory, set of capacities, and strategy for disaster readiness," *American journal of community psychology*, vol. 41, no. 1-2, pp. 127–150, 2008.

[47] K. Sherrieb, F. H. Norris, and S. Galea, "Measuring capacities for community resilience," *Social indicators research*, vol. 99, no. 2, pp. 227–247, 2010.

[48] A. Aiello, M. Young-Eun Khayeri, S. Raja, N. Peladeau, D. Romano, M. Leszcz, R. G. Maunder, M. Rose, M. A. Adam, C. Pain, *et al.*, "Resilience training for hospital workers in anticipation of an influenza pandemic," *Journal of Continuing Education in the Health Professions*, vol. 31, no. 1, pp. 15–20, 2011.

[49] D. Paton, B. Parkes, M. Daly, and L. Smith, "Fighting the flu: Developing sustained community resilience and preparedness," *Health Promotion Practice*, vol. 9, no. 4_suppl, pp. 45S–53S, 2008.

[50] J. R. Santos, M. J. Orsi, and E. J. Bond, "Pandemic recovery analysis using the dynamic inoperability input-output model," *Risk Analysis*, vol. 29, no. 12, pp. 1743–1758, 2009.

[51] C. Lian and Y. Y. Haimes, "Managing the risk of terrorism to interdependent infrastructure systems through the dynamic inoperability input–output model," *Systems Engineering*, vol. 9, no. 3, pp. 241–258, 2006.

[52] U. Soni, V. Jain, and S. Kumar, "Measuring supply chain resilience using a deterministic modeling approach," *Computers & Industrial Engineering*, vol. 74, pp. 11–25, 2014.

[53] T. J. Pettit, K. L. Croxton, and J. Fiksel, "Ensuring supply chain resilience: development and implementation of an assessment tool," *Journal of Business Logistics*, vol. 34, no. 1, pp. 46–76, 2013.

[54] T. J. Pettit, J. Fiksel, and K. L. Croxton, "Ensuring supply chain resilience: development of a conceptual framework," *Journal of business logistics*, vol. 31, no. 1, pp. 1–21, 2010.

[55] S. Torabi, M. Baghersad, and S. Mansouri, "Resilient supplier selection and order allocation under operational and disruption risks," *Transportation Research Part E: Logistics and Transportation Review*, vol. 79, pp. 22–48, 2015.

[56] M. Ouyang, L. Dueñas-Osorio, and X. Min, "A three-stage resilience analysis framework for urban infrastructure systems," *Structural Safety*, vol. 36, pp. 23–31, 2012.

[57] V. Dixit, N. Seshadrinath, and M. K. Tiwari, "Performance measures based optimization of supply chain network resilience: A NSGA-II + Co-Kriging approach," *Computers and Industrial Engineering*, vol. 93, pp. 205–214, 2016.

[58] D. Wang and W. H. Ip, "Evaluation and analysis of logistic network resilience with application to aircraft servicing," *IEEE Systems Journal*, vol. 3, no. 2, pp. 166–173, 2009.

[59] A. Munoz and M. Dunbar, "On the quantification of operational supply chain resilience," *International journal of production research*, vol. 53, no. 22, pp. 6736–6751, 2015.

[60] K. Zhao, A. Kumar, T. P. Harrison, and J. Yen, "Analyzing the resilience of complex supply network topologies against random and targeted disruptions," *IEEE Systems Journal*, vol. 5, no. 1, pp. 28–39, 2011.

[61] S. R. Cardoso, A. Paula Barbosa-Póvoa, S. Relvas, and A. Q. Novais, "Resilience metrics in the assessment of complex supply-chains performance operating under demand uncertainty," *Omega (United Kingdom)*, vol. 56, pp. 53–73, 2015.

[62] P. H. Longstaff and S.-U. Yang, "Communication management and trust: their role in building resilience to âĂIJsurprisesâĂİ such as natural disasters, pandemic flu, and terrorism," *Ecology and Society*, vol. 13, no. 1, p. 3, 2008.

[63] D. L. Martinez and T. K. Das, "Design of non-pharmaceutical intervention strategies for pandemic influenza outbreaks," *BMC public health*, vol. 14, no. 1, p. 1, 2014.

[64] N. M. Ferguson, D. A. Cummings, C. Fraser, J. C. Cajka, P. C. Cooley, and D. S. Burke, "Strategies for mitigating an influenza pandemic," *Nature*, vol. 442, no. 7101, p. 448, 2006.

[65] A. T. Newall, J. G. Wood, N. Oudin, and C. R. MacIntyre, "Cost-effectiveness of pharmaceutical-based pandemic influenza mitigation strategies," *Emerging Infectious Diseases*, vol. 16, no. 2, p. 224, 2010.

[66] S. Y. Ponomarov and M. C. Holcomb, "Understanding the concept of supply chain resilience," *The International Journal of Logistics Management*, vol. 20, no. 1, pp. 124–143, 2009.

[67] B. R. Tukamuhabwa, M. Stevenson, J. Busby, and M. Zorzini, "Supply chain resilience: definition, review and theoretical foundations for further study," *International Journal of Production Research*, vol. 53, no. 18, pp. 5592–5623, 2015.

[68] C. Roberta Pereira, M. Christopher, and A. Lago Da Silva, "Achieving supply chain resilience: the role of procurement," *Supply Chain Management: an international journal*, vol. 19, no. 5/6, pp. 626–642, 2014.

[69] A. J. Schmitt and M. Singh, "A quantitative analysis of disruption risk in a multi-echelon supply chain," *International Journal of Production Economics*, vol. 139, no. 1, pp. 22–32, 2012.

[70] M. Omer, R. Nilchiani, and A. Mostashari, "Measuring the resilience of the trans-oceanic telecommunication cable system," *IEEE Systems Journal*, vol. 3, no. 3, pp. 295–303, 2009.

[71] L. Chen and E. Miller-Hooks, "Resilience: An Indicator of Recovery Capability in Intermodal Freight Transport," vol. 46, no. 1, pp. 109–123, 2012.

[72] X. Zhang, E. Miller-Hooks, and K. Denny, "Assessing the role of network topology in transportation network resilience," *Journal of Transport Geography*, vol. 46, pp. 35–45, 2015.

[73] Sandhya Chandrasekaran and Swagata Banerjee, "Retrofit Optimization for Resilience Enhancement of Bridges under Multihazard Scenario," *Journal of Structural Engineering*, vol. 1, no. 2, pp. 1–12, 2013.

[74] E. J. Sutley, A. M. Asce, J. W. V. D. Lindt, M. Asce, and L. Peek, "Community-Level Framework for Seismic Resilience . II : Multiobjective Optimization and Illustrative Examples," vol. 18, no. 3, pp. 1–11, 2017.

[75] E. J. Sutley, A. M. Asce, J. W. V. D. Lindt, M. Asce, and L. Peek, "Community-Level Framework for Seismic Resilience . II : Multiobjective Optimization and Illustrative Examples," vol. 18, no. 3, pp. 1–11, 2017.

[76] M. Goerigk and H. W. Hamacher, "Optimisation models to enhance resilience in evacuation planning," *Civil Engineering and Environmental Systems*, vol. 32, no. 1-2, pp. 90–99, 2015.

[77] B. M. Ayyub, "Practical resilience metrics for planning, design, and decision making," *ASCE-ASME Journal of Risk and Uncertainty in Engineering Systems, Part A: Civil Engineering*, vol. 1, no. 3, p. 04015008, 2015.

[78] G. P. Cimellaro, A. M. Reinhorn, and M. Bruneau, "Seismic resilience of a hospital system," *Structure and Infrastructure Engineering*, vol. 6, no. 1-2, pp. 127–144, 2010.

[79] Y. Kim, Y.-S. Chen, and K. Linderman, "Supply network disruption and resilience: A network structural perspective," *Journal of operations Management*, vol. 33, pp. 43–59, 2015.

[80] A. M. Madni and S. Jackson, "Towards a conceptual framework for resilience engineering," *IEEE Systems Journal*, vol. 3, no. 2, pp. 181–191, 2009.

[81] R. L. Church and M. P. Scaparra, "Protecting critical assets: the r-interdiction median problem with fortification," *Geographical Analysis*, vol. 39, no. 2, pp. 129–146, 2007.

[82] R. Hemmecke, M. Köppe, J. Lee, and R. Weismantel, "Nonlinear integer programming," in *50 Years of Integer Programming 1958-2008*, pp. 561–618, Springer, 2010.